

Role of Magnetic Resonance Three-Dimensional Arterial Spin Labeling Perfusion in Diagnosis and Follow-Up of Viral Encephalitis in Children

Yang Cao ¹, Neng Xiao ², Shiteng Hu¹, Qiongmei Tang¹, Haijun Zhou¹

¹Department of Radiology, Chenzhou First People's Hospital, University of South China, Chenzhou, People's Republic of China; ²Department of Neurology, Chenzhou First People's Hospital, University of South China, Chenzhou, People's Republic of China

Correspondence: Yang Cao, Email cy_radiology@163.com

Objective: The aim of our study was to investigate the role of three-dimensional arterial spin labeling (3D-ASL) perfusion in the diagnosis and follow-up of children with viral encephalitis.

Methods: Twenty-five consecutive children with viral encephalitis and 25 healthy children of similar age were recruited for the study between 2017 and 2020. Conventional magnetic resonance imaging and 3D-ASL were performed for all subjects, and a color map of cerebral blood flow (CBF) was generated. The images were classified into three groups depending on the time points at which the magnetic resonance examinations were conducted, including the initial admission scan, inpatient review, and follow-up review. Clinical, neuroradiologic, and follow-up features were studied. The CBF values of the lesion area in the diseased brain group and the bilateral temporal cortex in the control group were measured and the differences between the two groups were compared.

Results: Perfusion was significantly increased in the acute cerebral disease group, and CBF and normalized cerebral blood flow (nCBF) were significantly higher than in the control group (124.5 vs 70.3 mL/100 g/min, 2.85 vs 1.36). Follow-up revealed that brain tissue perfusion in the lesion area of nine children decreased gradually after treatment, as their condition improved.

Conclusion: Brain tissue perfusion in children with viral encephalitis increases during the acute stage and decreases when the condition improves. 3D-ASL provides a reference for diagnosis and follow-up of viral encephalitis in children.

Keywords: pediatric, viral encephalitis, magnetic resonance, 3D arterial spin labeling

Introduction

Viral encephalitis (VE) is the most common infectious disease of the central nervous system (CNS) in children. Approximately 50–60% of surviving VE patients in developing countries have poor long-term prognoses.¹ Long-term persistent neurological and cognitive sequelae can occur, resulting in huge pressure and financial burdens on the patient's family and society. Early diagnosis and timely treatment are particularly important for improving prognosis.² The gold standard for VE diagnosis is the detection of viral antigens or specific antibodies in the cerebrospinal fluid (CSF), or the detection of viruses in brain tissue. However, the diagnosis rate of VE remains at only 52.5% even when modern laboratory testing techniques are used in large children's medical centers. The clinical diagnosis of this condition is primarily based on clinical signs and auxiliary examination data.³ Magnetic resonance imaging (MRI) has been widely used for the diagnosis and follow-up of VE, and FLAIR and DWI sequences can clearly reveal lesions.⁴ However, the MRI findings of VE overlap with those of other brain diseases, such as low-grade glioma, ischemic stroke, and mitochondrial encephalopathy (MELAS) with lactic acidosis and stroke-like episodes.^{5–7} When the clinical manifestations are atypical, differential diagnosis is difficult.

Three-dimensional arterial spin labeling (3D-ASL) is a magnetic resonance perfusion imaging technique that uses water protons in arterial blood as tracers to reflect tissue blood perfusion. This, in turn, can quickly determine the cerebral blood flow (CBF) of the target area, assess tissue blood perfusion, and provide objective and reliable imaging evidence

for the diagnosis of brain diseases. Currently, 3D-ASL is widely used to diagnose brain tumors, cerebrovascular diseases, MELAS, and other diseases.⁸⁻¹⁰ The application of 3D-ASL to adult viral encephalitis has not been reported to date, and existing findings may also be applicable to children. Therefore, we hypothesized that CBF changes occur in lesions in patients with childhood viral encephalitis, and that this change can be effectively captured by 3D-ASL.

This prospective study aimed to apply 3D-ASL technology to assess changes in tissue perfusion in the brains of children with VE and its evolutionary characteristics to investigate the role of 3D-ASL perfusion in the diagnosis and follow-up of children with VE.

Methods

Study Population

Twenty-five consecutive children with viral encephalitis and 25 healthy children of a similar age were recruited for this study between 2017 and 2020. Conventional MRI and 3D-ASL were performed in all subjects, a pseudo-color map of CBF was generated, and clinical data were collected by reviewing electronic medical records. The diagnostic criteria for VE refer to the Consensus Statement of the International Encephalitis Consortium:¹¹ major criterion (required): patients presenting to medical attention with altered mental status (defined as decreased or altered level of consciousness, lethargy, or personality change) lasting ≥ 24 h with no alternative cause identified. Minor criteria (2 required for possible encephalitis; ≥ 3 required for probable or confirmed encephalitis): 1) documented fever of ≥ 38 °C (100.4 °F) within 72 h before or after presentation. 2) Generalized or partial seizures not fully attributable to a pre-existing seizure disorder. 3) New-onset focal neurological findings. 4) CSF white blood cell count ≥ 5 /cubic mmd. 5) Abnormality of the brain parenchyma on neuroimaging, suggestive of encephalitis, which is either new from prior studies or appears acute at onset. 6) Abnormalities on electroencephalography are consistent with encephalitis and are not attributable to other causes. The exclusion criteria were as follows: 1) clinically suspected VE, but not definitively diagnosed; 2) VE was diagnosed based on clinical criteria, but MRI revealed no abnormal findings; 3) MRI had significant motion artifacts or unusable images; 4) 3D-ASL perfusion was not performed; and 5) vasoactive drugs were used.

All patients who met the above diagnostic criteria were hospitalized at the Chenzhou First People's Hospital and underwent routine MR and 3D-ASL examinations. Children who could not cooperate with the examination were orally administered 10% chloral hydrate orally (0.5 mL/kg).

The control group comprised of 25 healthy children. The inclusion criteria were as follows: 1) Match the control group according to the nearest neighbor principle at a ratio of 1:1 using propensity score matching (PSM) scores. The propensity scores were calculated based on age and sex. No substitution was allowed during the matching process and the matching tolerance was set to 0.05. Ultimately, 25 pairs of patients were matched. 2) The results of the neurological examination and MRI were normal. 3) No history of headache, epilepsy, head trauma, or other diseases affecting cerebral blood perfusion.

The images of the children were divided into three groups based on the different time points of the MRI examinations: initial admission, inpatient review, and follow-up review. (Initial admission scan, the first cranial MRI was performed after symptom onset; inpatient review, first review after hospitalization; follow-up review, review after discharge in two weeks).

This non intervention study was conducted in accordance with the principles of the Declaration of Helsinki. The Ethics Committee of Chenzhou First People's Hospital reviewed and approved the study. Because this study had no invasive examination and operation, the committee exempted informed consent.

Conventional MRI and 3D-ASL

MR images were acquired using a 1.5T MR (Signa HDxt, GE, USA) with a combined 8-channel coil of the head and neck. Conventional MR imaging includes the following: T1WI:TR/TE/TI=1750/24/720ms, matrix = 320×224, NEX = 2; T2WI: TR/TE=4000ms/105ms, matrix = 192×192, NEX = 1.5; T2-FLAIR: TR/TE/TI=8500/155/2100ms, matrix = 256×192, NEX = 1; DWI: TR/TE=4500/84.1ms, matrix = 160×160, NEX = 1; 3D-ASL:TR/TE=4932/10.6ms, post-labeling delay=1525ms, section thickness= 5 mm, NEX=3.

3D-ASL utilizes a fast spin-echo sequence to obtain perfusion image readout. The labeling duration was 1800ms, and the labeling plane was positioned 2–3 cm proximal to the imaging plane. A high level of background suppression was achieved by using four separate inversion pulses spaced around the pseudocontinuous labeling pulse. Multiarm spiral imaging was used with 8 arms and 512 points obtained on each arm, yielding a 3.49 mm² in-plane spatial resolution and 5-mm section thickness. Coverage included the entire cerebrum and most of the cerebellum. The acquisition time of the 3D-ASL was approximately 4 min 10s.

Quantitative CBF Measurement and Normalized CBF

The ADW 4.6 workstation (GE Healthcare) was used to process the original images to obtain CBF maps, which were registered and fused with T2-FLAIR as the anatomical reference. Reconstruction of ASL imaging is shown in the pseudo-color map, where the red area indicates high perfusion, the green area represents moderate perfusion, and the blue area indicates low perfusion. All imaging data were independently evaluated by two diagnostic imaging physicians (with 9 and 11 years of experience in pediatric imaging diagnosis), and agreement was reached through negotiation. Definition of abnormal MR signal: Slight hypo/hyper indicates that the lesion exhibits a slightly increased/decreased signal compared to normal tissue, and the boundary is unclear. Hypo/hyper was defined as a markedly increased/decreased signal compared with normal tissue with clear borders. Isointensity(ISO) represents normal signal readings.

Lesion area CBF: Regions of interest (ROIs) were drawn at the maximum level of abnormal perfusion in 3D-ASL. Three ROIs were selected for multiple lesions, and the average value was obtained. In the control group, two mirror-symmetrical circular ROIs were placed in the bilateral temporal cortex and the average was calculated (Figure 1A and B). It was approximately 40 mm².

Cerebellar hemisphere CBF: Two mirror-symmetrical ROIs were placed in the center of the bilateral cerebellar hemispheres and averaged to calculate normalized CBF (nCBF), which was defined as the lesion area in the patient group or the temporal lobe in the control group. The CBF value was divided by the mean CBF value of the cerebellar hemisphere (Figure 1C).

Statistical Analysis

Statistical analysis was performed using SPSS (version 23.0; IBM, Armonk, NY, USA) software to compare differences. The independent samples *t*-test was used for continuous variables with normal distribution; otherwise, the Mann-Whitney *U*-test was used. CBF and nCBF of the lesion area at the first inspection and review after hospitalization were compared; however, the discharge follow-up images were not compared with the former two because of the small

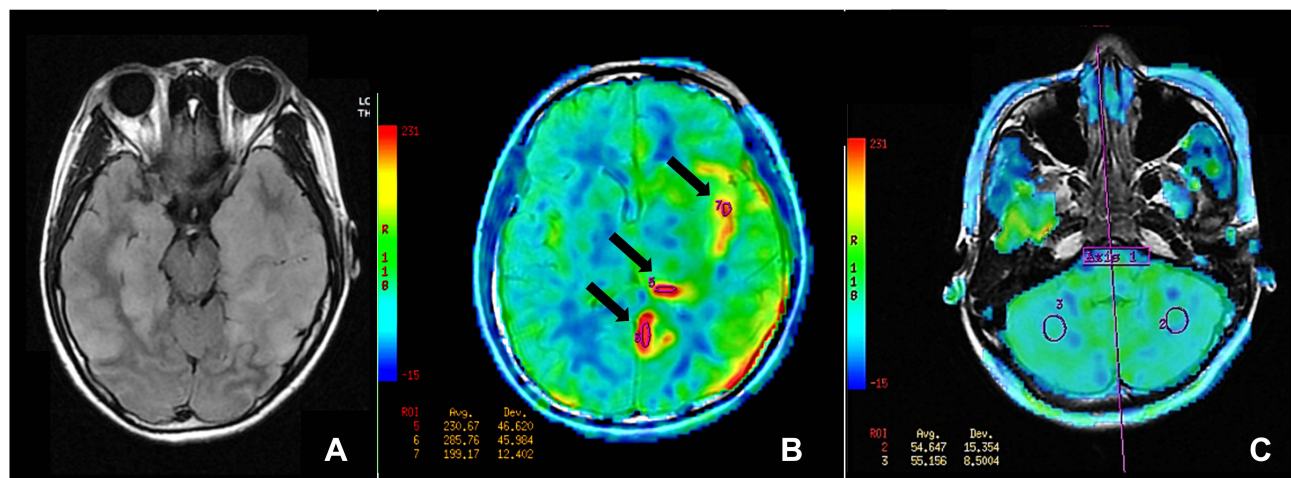


Figure 1 (A–C) Case 9, F, 14Y, initial admission scan (9 days after symptom onset). (A and B) Multiple lesions in bilateral cerebral hemispheres, basal ganglia and thalamus. (B and C): ROI site selection for CBF on ASL-CBF color maps.

Abbreviations: ROI, region of interest; CBF, cerebral blood flow; ASL, material spin labeling.

number of cases. Inter-observer variability was assessed using intra-class correlation coefficients (ICCs). The intraclass correlation coefficients were interpreted as follows: poor (<0.5), average (0.5–0.75), good (0.75–0.9), and excellent (>0.9).¹² Statistical significance was set at $P < 0.05$.

Result

Patient Population

Table 1 summarizes the demographic and clinical characteristics of the 25 children with viral encephalitis. The main clinical manifestations were fever ($n = 20$, 80%), convulsions ($n = 15$, 60%), headache ($n = 6$, 24%), disturbance of consciousness ($n = 6$, 24%), lethargy (6 cases, 24%), vomiting ($n = 5$, 20%), abnormal mental behavior ($n = 2$, 8%), physical movement disorder ($n = 2$, 8%), and language disorder ($n = 2$, 8%). The time from symptom onset to the first 3D-ASL scan ranged from 1 d to 10 days. Additionally, 9 patients underwent 3D-ASL review during hospitalization, and 2 underwent follow-up review after discharge.

Conventional MRI Findings

Table 2 summarizes the location and imaging findings of the lesions, with asymmetric bilateral and unilateral distributions observed in 14 (56%) and 11 (44%) patients, respectively. Its morphology is mostly irregular, and the affected areas include the temporal, frontal, parietal, insular, hippocampal, basal ganglia, and thalamus. A low signal was observed on T1WI (nine cases, 38%), a high signal on T2-FLAIR (21 cases, 84%), and a high signal on DWI (22 cases, 88%). The cerebellum was unaffected in all the cases.

Table 1 Summary of General Data and Clinical Manifestations of Children with Viral Encephalitis

Case No.	Age(yr)	Sex	Clinical Presentation	Time(Days) ^a
1	6	M	Fever, headache, vomiting, convulsions	1/9
2	6	M	Fever, disturbance of consciousness	3
3	3	F	Fever, convulsions, lethargy	2
4	11	M	Fever, headache, vomiting, disturbance of consciousness	8/17
5	2	F	Fever, vomiting, lethargy	7
6	4	F	Fever, convulsions	4
7	4	F	Convulsions	1/9
8	6	M	Fever, convulsion	2/7/40
9	14	F	Fever, headache, vomiting, lethargy, convulsions	9
10	3	F	Fever, convulsions, abnormal mental behavior	5/13
11	12	F	Fever, disturbance of consciousness	1
12	1	F	Fever, vomiting, convulsions	6
13	1	M	Fever, lethargy	5
14	4	M	Fever, language disorder	1/8
15	5	M	Fever, convulsions, disturbance of consciousness	10
16	5	M	Episodic behavioral abnormalities	1/9/25
17	11	F	Fever, abnormal mental behavior, headache, vomiting	5/16
18	9	F	Fever, disturbance of consciousness, Limbs weakness, convulsions	10
19	2	M	Vomiting, convulsions	3/7
20	1	M	Fever, lethargy language, disorder	6
21	2	F	Fever, headache	7
22	3	F	Fever, headache, convulsions	5
23	2	F	Fever, convulsions, lethargy	6
24	2	F	Convulsions	4
25	2	M	Fever, disturbance of consciousness, convulsions	7

Notes: ^aThe time from symptom onset to 3D-ASL evaluation.

Table 2 Initial Scan Findings After Admission in in Children with Viral Encephalitis

Case No.	Lesion Location	TIWI	T2/FLAIR	DWI	3D ASL
1	(R)FL, PL	Slight hypo	Hyper	Hyper	Hyper
2	(Bil.)PL	Iso	Slight hyper	Hyper	Hyper
3	(L)FL,TL,PL,OL	Iso	Slight hyper	Hyper	Hyper
4	(Bil.)Thalamus	Iso	Slight hyper	Slight hyper	Slight hyper
5	(Bil)FL,Brainstem	Slight hypo	Hyper	Slight hyper	Hyper
6	(L)TL	Iso	Iso	Hyper	Hyper
7	(R)TL	Iso	Iso	Slight hyper	Slight hyper
8	(R)FL,PL,OL	Iso	Slight hyper	Hyper	Hyper
9	(Bil)FL,TL,PL,OL,IL (L)Basal-ganglia,Thalamus	Slight hypo	Hyper	Hyper	Hyper
10	(Bil)FL,PL	Iso	Slight hyper	Hyper	Slight hyper
11	(Bil)FL,TL,PL,OL,	Slight hypo	Hyper	Hyper	Slight hyper
12	(Bil)FL,TL,PL, Basal-ganglia,Brainstem	Iso	Hyper	Hyper	Hyper
13	(Bil)FL,PL, Thalamus	Slight hypo	Hyper	Hyper	Hyper
14	Brainstem	Slight hypo	Hyper	Slight hyper	Hyper
15	(Bil)FL,TL,PL,Brainstem	Iso	Hyper	Hyper	Hyper
16	(L)FL,TL,PL, Basal-ganglia	Iso	Hyper	Hyper	Hyper
17	(Bil)Brainstem	Iso	Hyper	Hyper	Hyper
18	(Bil)TL, Thalamus, Brainstem	Slight hypo	Hyper	Hyper	Hyper
19	(Bil)Brainstem	Iso	Iso	Hyper	Slight hyper
20	(Bil)TL, Thalamus, Brainstem	Slight hypo	Hyper	Hyper	Hyper
21	(L)FL, Thalamus	Iso	Hyper	Iso	Slight hyper
22	(L)PL	Iso	Hyper	Iso	Slight hyper
23	(L)FL,PL,IL	Slight hypo	Hyper	Hyper	Hyper
24	(R)PL	Iso	Iso	Hyper	Hyper
25	(Bil)Basal-ganglia,(R)FL	Iso	Hyper	Iso	Slight hyper

Abbreviations: R, indicates right; L, left; Bil, bilateral; FL, frontal lobe; TL, temporal lobe; PL, parietal lobe; OL, occipital lobe; IL, insular lobe; hyper, hyperintensity or hyperperfusion; hypo, hypointensity or hypoperfusion; Iso, isointensity.

Quantitative Measurement Features of 3D-ASL

Macroscopically, all 25 children with VE exhibited markedly increased perfusion during the first 3D-ASL examination (Figure 1B). Nine children were reviewed during hospitalization, and brain tissue perfusion in the lesion area decreased as the disease symptoms improved (Figure 2A–H). Two patients were followed-up after discharge, and the lesions exhibited slight hypoperfusion. For the repeatability of CBF values between the two observers, the intra-group correlation coefficient was 0.89 in the first inspection group, 0.88 in the review group, 0.79 in the follow-up group, and 0.85 in the control group was calculated. The mean CBF and nCBF values in the lesion area were: first 3D-ASL (124.5 ± 41.4 mL/100 g/min, 2.81 ± 1.08), follow-up after hospitalization (67.6 ± 17.2 mL/100 g/min, 1.63 ± 0.51); follow-up after discharge (58.5 ± 33.2 mL/100 g/min; 1.03 ± 0.35); control group (70.3 ± 6.6 mL/100 g/min; 1.36 ± 0.19) (Table 3). The CBF and nCBF values of the lesion area in the initial admission scan were significantly higher than those in the inpatient ($P=0.001$) and control ($P=0.001$) groups. The inpatient review was slightly higher than the control group ($P=0.38$), whereas the follow-up review was not compared due to the small number of cases (Figure 2), with no statistical significance (Figure 3). Nine patients were reviewed after treatment and the nCBF values of the lesions gradually decreased (Figure 4).

Discussion

The results of our study demonstrated that CBF changes occur in the lesions of patients with childhood viral encephalitis, and this change can be effectively captured by 3D-ASL. In this group of children with VE, conventional MRI remains a crucial test for diagnosing VE. The 3D-ASL quantitative perfusion feature is that the nCBF value of the lesion area in the early stage of the disease is significantly higher than that of normal children (2.81 ± 1.08 vs 1.36 ± 0.19 , $P < 0.05$). After

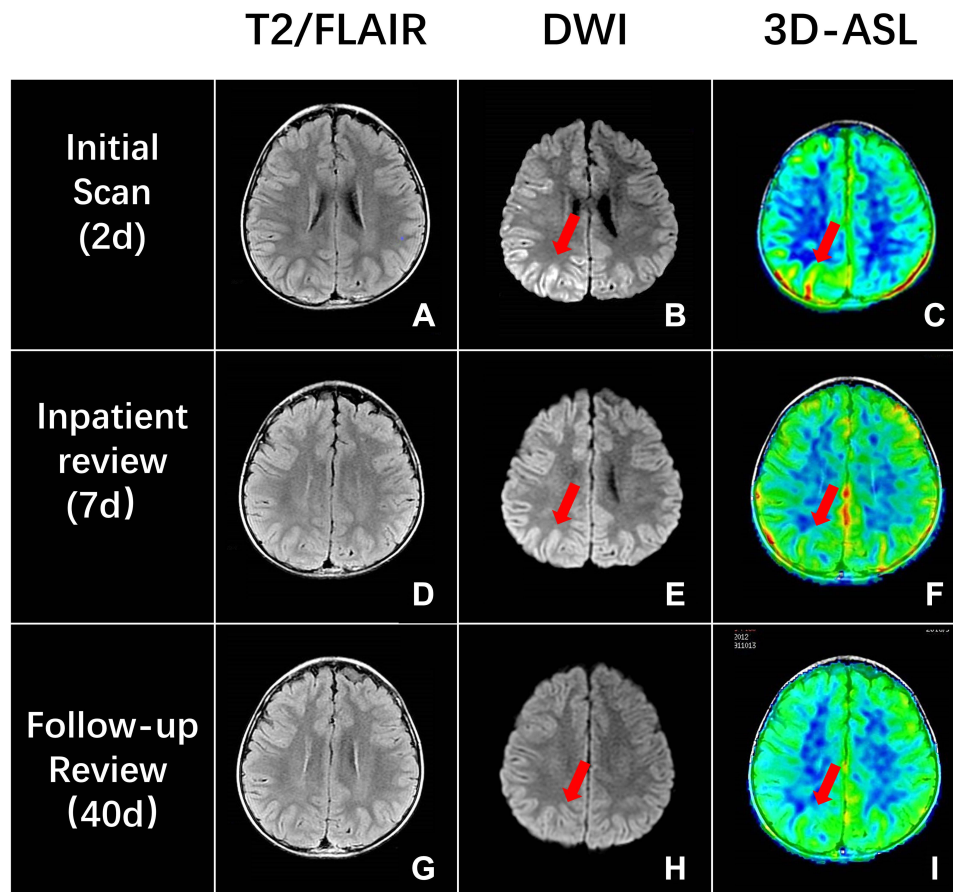


Figure 2 (A–H): Case 8, a 6-year-old male patient. T2-FLAIR (A, D and G) revealed no abnormal signal; DWI (B, E and H) revealed increased local cortical signal in the right parietal lobe. 3D-ASL (C, F and I): Serial follow-up 3D-ASL shows dynamic changes in the involved area on the initial scan (2d), inpatient review (7d), and follow-up review (40d), respectively (red arrows).

Abbreviations: DWI, diffusion-weighted imaging, 3D-ASL, three-dimensional arterial spin labeling.

effective treatment, the nCBF value of the lesion area gradually decreased as the disease improves (2.81 ± 1.08 vs 1.63 ± 0.51 , $P < 0.05$). After discharge, the nCBF value of the lesion area was slightly lower than that of normal children (1.03 ± 0.35 vs 1.36 ± 0.19). These perfusion characteristics may provide clinicians with more useful information for determining diagnosis and assessing prognosis and deserve further study.

Few studies on VE perfusion in children have been conducted to date, and the mechanism of CBF changes in viral encephalitis lesions has not been fully explained. Some researchers have speculated that vasculitis due to direct viral invasion or immune-mediated injury in the acute phase may lead to vasodilation, which, in turn, increases metabolism and local CBF.¹³ In the chronic phase, focal slightly hypoperfused ROIs may be the result of excessive neuronal damage

Table 3 Comparison of the Values of CBF and NCBF in the Lesion Area of the Disease Group, the Reexamination Group, the Follow-Up Group and the Control Group

	Initial Scan	Inpatient Review	Follow-Up Review	Control Group
NO.	25	9	2	25
SEX(M/F)	11/14	5/2	2/0	12/13
Age(yr)	5.5 ± 3.92	5.7 ± 3.23	5.5 ± 0.7	5.45 ± 3.89
CBF(mL/100g/min)	124.5 ± 39.2	67.6 ± 17.2	58.5 ± 33.2	70.3 ± 6.6
nCBF	2.85 ± 1.02	1.63 ± 0.51	1.03 ± 0.35	1.36 ± 0.19

Abbreviations: CBF, cerebral blood flow; nCBF, normalized CBF.

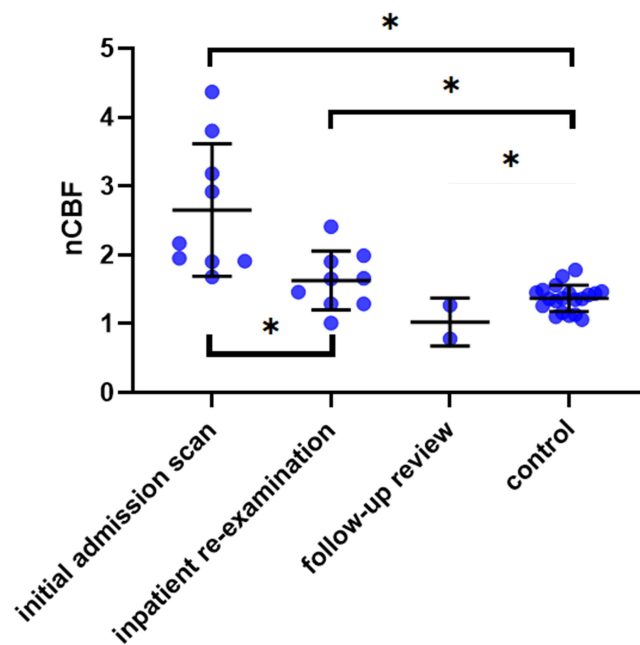


Figure 3 Scatter plot of nCBF values in the initial scan, inpatient review, follow-up review and control group, respectively. *Signifies P<0.05. **Abbreviation:** nCBF, relative cerebral blood flow.

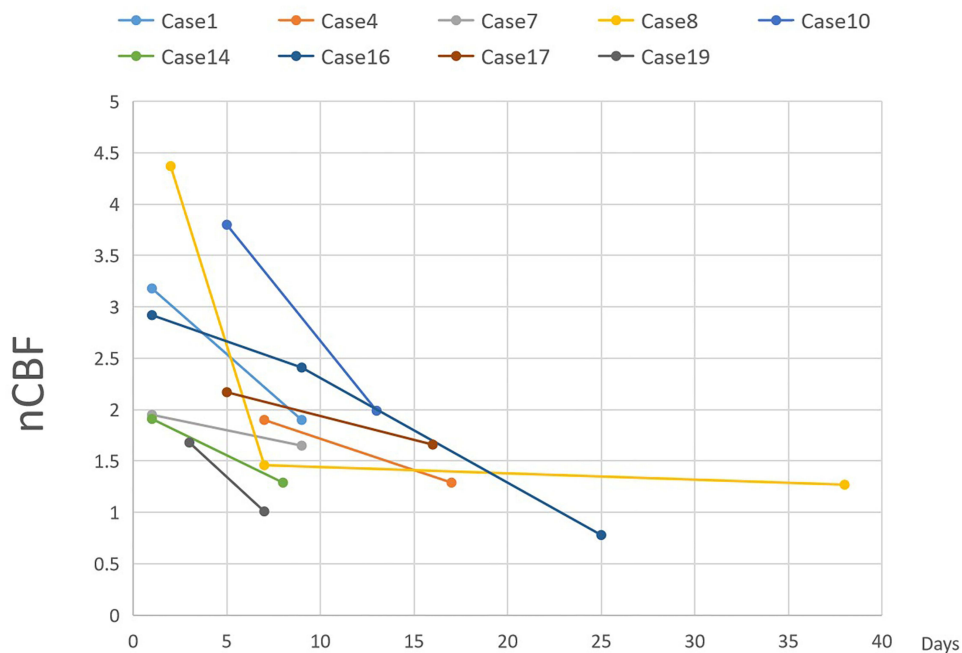


Figure 4 Time course of mean changes in CBF for lesions at different time points in 9 review and follow-up VE cases. The nCBF value of the lesions gradually decreased after treatment in 9 case series. **Abbreviations:** CBF, cerebral blood flow; nCBF, relative CBF; VE, viral encephalitis.

and loss of the brain parenchyma caused by a series of direct viral and indirect immune-mediated responses.¹⁴ Noguchi et al¹⁵ reported the application of ASL-MRI in central nervous system infections (only ten cases of VE). Additionally, the results revealed that the visual assessment of VE lesions showed ASL hyperperfusion; however, no quantitative analysis was performed. It is generally believed that excessive neuronal damage and brain parenchyma loss may cause corresponding brain dysfunction in children, even the formation of softening focus in the long term and induce

seizures. These long-term effects need to be confirmed by a large sample of long-term follow-up data. The quantitative value of ASL-CBF is expected to improve the diagnosis, management, follow-up and complication prevention of children with viral encephalitis in the future. Wong¹³ and other researchers believe that changes caused by brain tissue perfusion in the acute phase of VE in children are related to epileptic seizures and prognosis. If CBF returned to normal in the subacute phase, it usually indicated that neurological function recovered well after one year in the acute phase.

3D-ASL perfusion facilitates the differential diagnosis of cerebral infarction, Moyamoya disease, MELAS, post-ictal migraine, and low-grade gliomas, particularly during the acute phase. Acute cerebral infarction lesions exhibit hypoperfusion, which can be reliably differentiated from early VE.⁹ MELAS was initially misdiagnosed as VE⁷ and both showed hyperperfusion. Hyperperfusion in MELAS is primarily located in the cortical area.¹⁶ The perfusion performance of low-grade gliomas is similar to that of early VE.¹⁷ Both showed hyperperfusion on 3D-ASL; however, hyperperfusion in lower-grade gliomas was not as high as that in VE, and they could be identified based on clinical manifestations, medical history, and lesion location. The clinical symptoms of migraine in children are similar to those of VE, and ASL perfusion imaging shows hypoperfusion associated with homolateral vasospasm, which can be differentiated from hyperperfusion of VE.¹⁸ In conclusion, 3D-ASL perfusion characteristics have good application value for diagnosis, efficacy evaluation, and prognosis monitoring of VE in children.

Several methods are currently used to quantitatively measure CBF, including single-photon emission computed tomography, positron emission tomography, computed tomography, and magnetic resonance perfusion imaging. However, all these methods use a tracer kinetic model, which requires the injection of a contrast agent to determine the CBF value. This involves the risk of trauma and side effects of the contrast agent, is expensive, and results in radiation exposure.^{19–21} 3D-ASL has the advantages of non-invasiveness, non-radiation, simplicity, and reproducibility and has broad application prospects in children's brain diseases.

Limitations of this study: First, The sample size was relatively small. Second, owing to the low positive rate of etiological examinations, etiological classification was not performed in this study. Finally, the post-label delay time (PLD) of 3D-ASL in this study was 1525 ms to ensure consistent scanning parameters. However, some researchers believe that the optimal PLD of 3D-ASL differs in children of different ages.²² Whether the use of different PLDs affects the evaluation of changes in VE brain microcirculation requires further investigation.

Conclusions

3D-ASL imaging can detect changes in the cerebral microcirculation in children with VE, and hyperperfusion in the lesion area provides a new imaging reference for diagnosis. The nCBF value measured using 3D-ASL may be useful for evaluating efficacy and monitoring the prognosis of children with VE.

Funding

This work was supported by the Chenzhou Science and Technology Bureau Technology Innovation Guidance Special Project (ZDYF2020074) and In-hospital Scientific Research Project of Chenzhou First People's Hospital (N2019-018).

Disclosure

The authors declare no conflicts of interest in this work.

References

1. Feng G, Zhou L, Li F, et al. Predictors of outcome in clinically diagnosed viral encephalitis patients: a 5-year prospective study. *BioMed Res Int*. 2020;2020:2832418. doi:10.1155/2020/2832418
2. Britton PN, Eastwood K, Paterson B, et al. Consensus guidelines for the investigation and management of encephalitis in adults and children in Australia and New Zealand. *Intern Med J*. 2015;45:563–576. doi:10.1111/imj.12749
3. Ai J, Xie Z, Liu G, et al. Etiology and prognosis of acute viral encephalitis and meningitis in Chinese children: a multicentre prospective study. *BMC Infect Dis*. 2017;17:494. doi:10.1186/s12879-017-2572-9
4. Jayaraman K, Rangasami R, Chandrasekharan A. Magnetic resonance imaging findings in viral encephalitis: a pictorial essay. *J Neurosci Rural Pract*. 2018;9:556–560. doi:10.4103/jnrp.jnrp_120_18
5. Panagopoulos D, Themistocleous M, Apostolopoulou K, et al. Herpes simplex encephalitis initially erroneously diagnosed as glioma of the cerebellum: case report and literature review. *World Neurosurg*. 2019;129:421–427. doi:10.1016/j.wneu.2019.06.158

6. Tsuboguchi S, Wakasugi T, Umeda Y, et al. Herpes simplex encephalitis presenting as stroke-like symptoms with atypical MRI findings and lacking cerebrospinal fluid pleocytosis. *Rinsho Shinkeigaku*. 2017;57:387–390. doi:10.5692/clinicalneurolog.cn-001033
7. Gooriah R, Dafalla BE, Venugopalan TC. Led astray: MELAS initially misdiagnosed as herpes simplex encephalitis. *Acta Neurol Belg*. 2015;115:789–792. doi:10.1007/s13760-014-0416-6
8. Kang XW, Xi YB, Liu TT, et al. Grading of glioma: combined diagnostic value of amide proton transfer weighted, arterial spin labeling and diffusion weighted magnetic resonance imaging. *BMC Med Imaging*. 2020;20:50. doi:10.1186/s12880-020-00450-x
9. Su H, Su S, Zhang X, et al. Application of arterial spin labeling and susceptibility weighted imaging in the diagnosis of ischemic cerebrovascular diseases. *Int J Clin Exp Pathol*. 2020;13:3052–3059.
10. Wang R, Hu B, Sun C, et al. Metabolic abnormality in acute stroke-like lesion and its relationship with focal cerebral blood flow in patients with MELAS: evidence from proton MR spectroscopy and arterial spin labeling. *Mitochondrion*. 2021;59:276–282. doi:10.1016/j.mito.2021.06.012
11. Venkatesan A, Tunkel AR, Bloch KC, et al. Case definitions, diagnostic algorithms, and priorities in encephalitis: consensus statement of the international encephalitis consortium. *Clin Infect Dis*. 2013;57:1114–1128. doi:10.1093/cid/cit458
12. Koo TK, Li MY. A guideline of selecting and reporting intraclass correlation coefficients for reliability research. *J Chiropr Med*. 2016;15:155–163. doi:10.1016/j.jcm.2016.02.012
13. Wong AM, Yeh CH, Lin JJ, et al. Arterial spin-labeling perfusion imaging of childhood encephalitis: correlation with seizure and clinical outcome. *Neuroradiology*. 2018;60:961–970. doi:10.1007/s00234-018-2062-9
14. Chucair-Elliott AJ, Conrady C, Zheng M, et al. Microglia-induced IL-6 protects against neuronal loss following HSV-1 infection of neural progenitor cells. *Glia*. 2014;62:1418–1434. doi:10.1002/glia.22689
15. Noguchi T, Yakushiji Y, Nishihara M, et al. Arterial spin-labeling in central nervous system infection. *Magn Reson Med Sci*. 2016;15:386–394. doi:10.2463/mrms.mp.2015-0140
16. Li R, Xiao HF, Lyu JH, et al. X-Differential diagnosis of mitochondrial encephalopathy with lactic acidosis and stroke-like episodes (MELAS) and ischemic stroke using 3D pseudocontinuous arterial spin labeling. *J Magn Reson Imaging*. 2017;45:199–206. doi:10.1002/jmri.25354
17. Xiao HF, Chen ZY, Lou X, et al. Astrocytic tumour grading: a comparative study of three-dimensional pseudocontinuous arterial spin labeling, dynamic susceptibility contrast-enhanced perfusion-weighted imaging, and diffusion-weighted imaging. *Eur Radiol*. 2015;25:3423–3430. doi:10.1007/s00330-015-3768-2
18. Cadiot D, Longuet R, Bruneau B, et al. Magnetic resonance imaging in children presenting migraine with aura: association of hypoperfusion detected by arterial spin labeling and vasospasm on MR angiography findings. *Cephalalgia*. 2018;38:949–958. doi:10.1177/0333102417723570
19. Pagani M, Salmaso D, Jonsson C, et al. Regional cerebral blood flow as assessed by principal component analysis and (99m)Tc-HMPAO SPET in healthy subjects at rest: normal distribution and effect of age and gender. *Eur J Nucl Med Mol Imaging*. 2002;29:67–75. doi:10.1007/s00259-001-0676-2
20. Ahlgren A, Wirestam R, Lind E, et al. A linear mixed perfusion model for tissue partial volume correction of perfusion estimates in dynamic susceptibility contrast MRI: impact on absolute quantification, repeatability, and agreement with pseudo-continuous arterial spin labeling. *Magn Reson Med*. 2017;77:2203–2214. doi:10.1002/mrm.26305
21. Tian B, Liu Q, Wang X, et al. Chronic intracranial artery stenosis: comparison of whole-brain arterial spin labeling with CT perfusion. *Clin Imaging*. 2018;52:252–259. doi:10.1016/j.clinimag.2018.08.005
22. Tang S, Liu X, He L, et al. Application of postlabeling delay time in 3-dimensional pseudocontinuous arterial spin-labeled perfusion imaging in normal children. *J Comput Assist Tomogr*. 2019;43:697–707. doi:10.1097/RCT.0000000000000911

International Journal of General Medicine

Dovepress

Publish your work in this journal

The International Journal of General Medicine is an international, peer-reviewed open-access journal that focuses on general and internal medicine, pathogenesis, epidemiology, diagnosis, monitoring and treatment protocols. The journal is characterized by the rapid reporting of reviews, original research and clinical studies across all disease areas. The manuscript management system is completely online and includes a very quick and fair peer-review system, which is all easy to use. Visit <http://www.dovepress.com/testimonials.php> to read real quotes from published authors.

Submit your manuscript here: <https://www.dovepress.com/international-journal-of-general-medicine-journal>